


Original article

Extreme Events of Marine Heat Waves off the Eastern Coast of Kamchatka Peninsula and in the Adjacent Areas under Conditions of Modern Global Warming

I. D. Rostov , E. V. Dmitrieva, I. A. Zhabin

*V. I. Il'ichev Pacific Oceanological Institute, Far Eastern Branch of Russian Academy of Sciences,
Vladivostok, Russian Federation*

 rostov@poi.dvo.ru

Abstract

Purpose. The purpose of the study is to determine the characteristics and trends of inter-annual variability of marine heat wave parameters off the Kamchatka Peninsula eastern coast and in the adjacent areas over the past four decades and to analyze their cause-and-effect relationships with the large-scale and regional processes in the ocean and atmosphere in the context of global warming, as well as to investigate the possible role of coastal wind upwelling in the chain of events of a large-scale environmental disaster in the study region in the fall 2020 under conditions of intensification of marine heat waves and outbreak of harmful algal blooms.

Methods and Results. Standard methods for identifying the variability of marine heat waves and for determining the amplitude-frequency parameters at the regular grid nodes were used to analyze the NOAA climate data array. The results enabled detailed characterization of the spatiotemporal variability of marine heat waves in the region under study including the frequency of events, their duration, intensity, integral indicators (cumulative intensity and composite intensity index), as well as the trends in inter-annual and seasonal variations. The cases of wind-driven upwelling of deep-sea waters in the coastal zone accompanied by a surge in chlorophyll *a* concentration on the ocean surface during the harmful algal bloom outbreak were also identified.

Conclusions. The marine heat wave events developed against the background of stable positive trends in sea surface temperature. During the last two decades of global warming, a significant increase in all the marine heat wave indicators has been observed. Statistically significant correlations were identified between fluctuations in various marine heat wave parameters and changes in characteristics of anomalies of the surface air temperature field, geopotential height of the 500 mbar isobaric surface as well as climate indices indicating the local and remote influence of large-scale atmospheric processes. During the outbreak of harmful algal bloom off the Kamchatka coast observed after the marine heat waves impact, an increase in wind upwelling in the coastal zone was noted that facilitated the entry of nutrients and dinoflagellates into the photic layer, and also an increase in their numbers and chlorophyll *a* concentration. The conducted studies confirm the assumption about the role of extreme marine heat waves in the chain of events of the environmental disaster that took place in the region under study in the fall 2020.

Keywords: northwestern Pacific Ocean, Kamchatka, climate change, marine heat waves, upwelling, chlorophyll concentration, climate indices, correlations

Acknowledgments: This work was conducted under the state assignment of POI FEB RAS, titled “Response and Potential Change of Coastal Ecosystems of Kamchatka under Conditions of Global Climatic and Local Catastrophic Impacts” (registration number 124072200009-5).

For citation: Rostov, I.D., Dmitrieva, E.V. and Zhabin, I.A., 2025. Extreme Events of Marine Heat Waves off the Eastern Coast of the Kamchatka Peninsula and in the Adjacent Areas under Conditions of Modern Global Warming. *Physical Oceanography*, 32(4), pp. 446-463.

© 2025, I. D. Rostov, E. V. Dmitrieva, I. A. Zhabin

© 2025, Physical Oceanography



Introduction

Amid ongoing global warming, extreme climatic phenomena in both the atmosphere and ocean are becoming increasingly frequent, prolonged, and intense. In the ocean, such phenomena include marine heatwaves (MHWs), recognized as one of the most serious extreme events caused by climate change [1]. These waves can be defined as prolonged, discrete, anomalously warm events characterized by duration, intensity, rate of evolution, and spatial extent [1, 2]. Qualitatively, MHWs are defined [3] as discrete periods of prolonged anomalously warm surface water in a specific location, while quantitative definitions are based on ocean temperatures exceeding fixed seasonally varying or cumulative thresholds that differ across regions. Based on a standardized methodology [2], most studies define an MHW event as a prolonged anomalously warm period at the ocean surface lasting at least five consecutive days with temperatures above the 90th percentile for a chosen time period.

The occurrence of MHWs can be triggered by a combination of local oceanic and atmospheric processes, such as air-sea heat fluxes and horizontal advection. These processes can be modulated by large-scale climate variability through teleconnections and interactions [3, 4]. MHWs are typically identified using sea surface temperatures (SSTs), although they can extend to greater depths. Alongside extreme thermal anomalies, the opposite phenomena – extreme marine cold spells – are also periodically observed, with their metrics decreasing in most regions [1, 5], though their intensity may increase in some locations.

Over the past few decades, MHWs have been observed in all ocean basins [1, 2, 4], and their frequency and intensity are projected to increase throughout the 21st century [5]. Notably, over the last 40 years, the average intensity of MHWs in the Arctic marginal seas has become comparable to that observed in other regions of the World Ocean [6]. MHW events can last from several days to several months and cover tens to hundreds of kilometers of water area. They pose a significant threat to marine ecosystems, coastal biological communities, and the economies of coastal regions [2, 6, 7], but can also create favorable conditions for the spread of invasive species.

The factors determining the onset and termination of individual MHW events are diverse and can vary depending on the region, season, and event scale [4]. Oceanic advection plays a key role in regulating the characteristics of small-scale MHWs, while atmospheric processes are the primary driver for larger-scale MHW events. Generally, as the spatial scale increases, MHWs become less intense, occur less frequently, and last longer [8]. During periods of extreme warming, a weakening of vertical water mixing processes and enhanced stratification are observed, reducing the supply of nutrients to the surface, causing water acidification, and decreasing dissolved oxygen levels to critical values [9, 10].

The main risks associated with the impact of MHWs on marine biota [10] arise from disruptions to natural habitat conditions and life cycles of aquatic organisms when their adaptive limits are exceeded. This also leads to disruptions in food

chains, deterioration of oxygen conditions, and the emergence of toxicological threats associated with harmful algal blooms (HABs) [11]. Temperature and nutrient supply are key factors controlling ocean productivity [12, 13]. According to research [14], MHWs can both decrease chlorophyll concentration (an indicator of phytoplankton biomass) [9] and promote its increase across different latitudes. The magnitude of the chlorophyll response to temperature rise increases with the intensity and duration of the MHWs and the rate of nutrient supply to the upper mixed layer. However, the links between these processes are complex and ambiguous.

Numerous studies have shown that MHWs have caused mass HAB events in various regions around the world [15]. Such events have become increasingly frequent in recent decades and have expanded both temporally and spatially, exerting unprecedented impacts on marine ecosystems [1, 16, 17]. In some cases, these phenomena have led to catastrophic consequences for coastal aquaculture and fisheries. For instance, in late September – early October 2020, an ecological disaster occurred in the waters of Avacha Gulf and other areas along the southeastern coast of Kamchatka. It was accompanied by massive phytoplankton development and an anomalous increase in chlorophyll a concentration. These changes led to the appearance of foam, films of biogenic surfactants on the water surface, and mass mortality of marine organisms (up to 95% of benthos) [18, 19]. Research indicated that the cause was a massive and prolonged bloom of the dinoflagellate species *Karenia selliformis* [19], whose abundance closely correlated with chlorophyll a concentration but was not linked to anthropogenic eutrophication [18, 20], characteristic of Avacha Bay adjacent to Avacha Gulf. The HAB lasted two months and covered an extensive area exceeding 300×100 km [19].

Among the probable factors contributing to this phenomenon were strong positive water temperature anomalies, which can be regarded as intense MHWs [15]. Other contributing factors include the supply of nutrients from deep water layers due to wind-wave mixing triggered by the passage of three deep cyclones between September 19 and October 7, 2020 [21], as well as the influence of Typhoon Dolphin, which may have intensified these processes. Additionally, the influence of wind-driven upwelling, promoting the rise of dinoflagellates to the surface, was considered as a possible cause of the HAB outbreak [19], but this hypothesis was not conclusively confirmed during the study. Similar phenomena associated with massive HABs are known as “red tides” and have been recorded in Kamchatka bays before [21]. A year later, in September – November 2021, similar events occurred in the southern part of the region, off the Pacific coast of Hokkaido, where intense MHWs were also observed [16]. A massive dinoflagellate bloom [20] was recorded in this region as well, accompanied by marine organism mortality. These events were linked to features of mesoscale water dynamics and intensification of horizontal and vertical mixing processes that followed intense and extensive MHW manifestations in the area [15]. Overall, the retrospective

analysis of toxic HAB events and laboratory experiments confirm the link between sharp water temperature increases and increased toxin production rates [17].

It should be noted, however, that the multifactorial biological impacts on marine ecosystems associated with various MHW characteristics can vary significantly. The mechanisms of these processes, as well as their causal relationships, remain insufficiently studied [15, 22]. It has been established that the ecosystem response depends significantly on the duration, intensity, and timing of extreme events [23]. At the same time, reliable data on the frequency of HAB occurrences and on MHW characteristics off the eastern coast of Kamchatka, similar to those available for the Bohai Sea [16], are lacking. Overall, in recent years, a certain dependence of HAB occurrence and dynamics on MHW characteristics has been observed in both the northeastern and northwestern Pacific Ocean.

Several key factors influencing HAB development can be highlighted:

- more frequent HAB outbreaks are associated with anomalously warm thermal conditions arising from MHW influence [17, 20]. However, subsequently, these conditions can exert a negative impact on sustaining such algal populations, acting as a stressor for their growth [24];
- in years with “red tides” (HAB period), the total number of days with MHWs is generally higher than in years without them. “Red tides” occur more frequently in areas with higher MHW frequency and duration compared to neighboring waters [25];
- even in locations where such algae are rare, recurrent HAB events can occur in subsequent years following an outbreak [20];
- formation of areas of extreme temperature anomalies on the ocean surface and enhanced stratification caused by MHWs one month [15] or more prior to the onset of HABs facilitate the initiation and acceleration of HAB development processes;
- HAB outbreaks occur when algae encounter optimal ecological conditions [15]. Processes such as wind-wave mixing, upwelling, horizontal advection, and mesoscale water dynamics, leading to the influx of nutrients from deep layers into the photic zone, are necessary for phytoplankton nutrition and sustaining HABs [17, 18];
- expansion of the area affected by HABs is linked to the deepening of the mixed surface layer and the entrainment of nutrients from river runoff [15, 18, 21] and adjacent waters.

The marine areas adjacent to the eastern coast of the Kamchatka Peninsula represent one of the most dynamically active and productive regions of the Pacific Ocean, providing essential conditions for the reproduction and fishery of numerous fish species and other aquatic organisms. At the turn of the 20th – 21st centuries, the study area was dominated by unidirectional trends in thermal conditions towards increasing water and air temperatures, primarily due to changes in heat exchange with the atmosphere, manifested in ice cover characteristics,

thermohaline structure, and water heat content [26]. These processes are characterized by significant spatiotemporal variability and exert a noticeable influence on the ecological state and biota of the region. The waters of the region exhibited the highest warming rate within the entire Pacific basin, with the trend contribution to the total variance of annual mean SST reaching 30–40% [26]. The largest trends in air temperature (T_a) and SST were observed in the western Bering Sea and off the eastern coast of Kamchatka [27]. The features of their interannual variability are determined by surface forcing and the internal dynamics of the ocean. They include seasonal changes, as well as decadal and multidecadal oscillations superimposed on monotonic trends under changing climatic regimes and specific phases of global warming.

Currently, the metrics of MHW events – quantitative indicators (such as intensity, duration, frequency, spatial coverage [2]), their statistical characteristics, as well as cause-and-effect relationships with atmospheric and oceanic processes in the northwestern Pacific region off the eastern coast of Kamchatka remain insufficiently studied.

The aim of this work is to determine the characteristics and trends of interannual variability of MHW parameters off the eastern coast of Kamchatka and adjacent areas, analyze cause-and-effect relationships with large-scale and regional processes in the ocean and atmosphere over the past 40 years, and investigate the potential role of coastal wind-driven upwelling in the chain of events of the large-scale ecological disaster in the study region amid intensifying MHWs and the HAB outbreak.

Data and methods

The study area is bounded by coordinates 51–63° N, 156–180° E, and the temporal period covers four decades from 1982 to 2023. Optimally interpolated daily SST data (NOAA-OI SST V2) on a $0.25^\circ \times 0.25^\circ$ grid, available at <https://www.psl.noaa.gov/data/gridded/data.noaa.oisst.v2.highres.html>, and the standard MHW identification method [2] are used in the present paper. An MHW event was defined as an anomalously warm phenomenon on the ocean surface lasting at least five consecutive days (two consecutive events separated by less than three days are considered a single event) with SSTs exceeding the 90th percentile, based on a 30-year baseline climatological period (1988–2018) using Matlab software [28]. According to the method [2], the 90th percentile was calculated for each calendar day using daily SST values within an 11-day window centered on the data across all years within the climatological period and smoothed by applying a 31-day moving average. To describe, comparatively analyze, and classify MHW characteristics in each grid cell and averaged over the region, various metrics [2] were calculated, defined based on the extent to which actual temperature values exceed the local climatology of the 90th percentile for the baseline period [22]:

– frequency – the number of MHW events per year (F);

- duration – the number of days between the start and end of an MHW event period when SST exceeds the 90th percentile threshold (D , days);
- intensity – the deviation of the daily mean SST relative to the 90th percentile of the baseline period on a selected day (I , °C);
- mean intensity, representing the average intensity (temperature anomaly) for the entire MHW event under consideration (I_{mean} , °C);
- maximum intensity – the largest temperature anomaly during the MHW event period (I_{max} , °C);
- cumulative intensity – an indicator summing the temperature anomaly values over the MHW event duration (I_{cum} , °C);
- cumulative intensity (composite) index, which integrates the frequency (number) of events, their intensity, and duration over the entire period (ICI, °C·days).

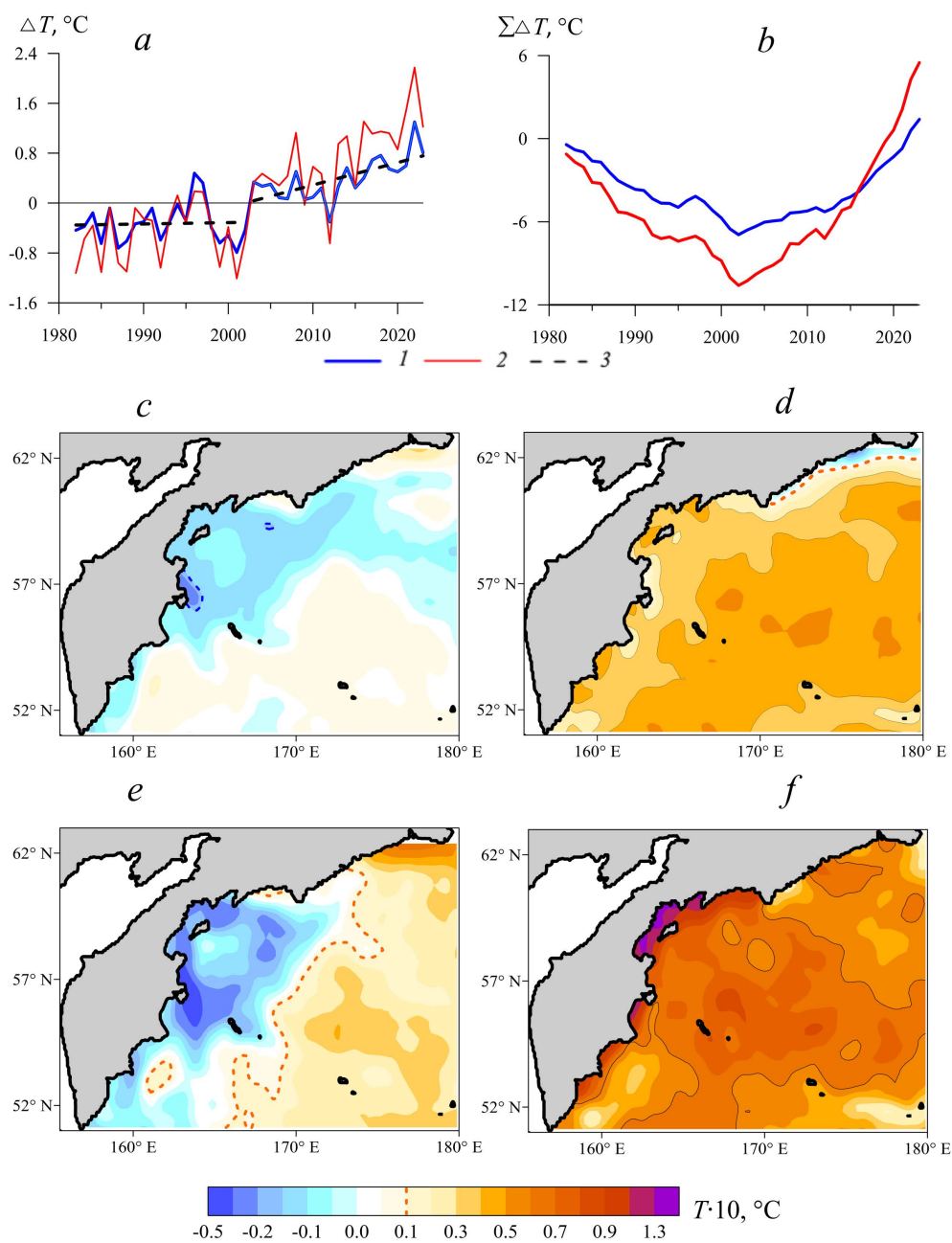
Reanalysis data for surface air temperature (T_a), pressure, and wind, along with time series of CI (*AMO*, *NPGO*, *PDO*, *SOI*, *WP*, *NINO.WEST*) [26, 29] were obtained from NOAA websites: <https://psl.noaa.gov/data/gridded/index.html> and <https://psl.noaa.gov/data/climateindices/list/>. Satellite data on chlorophyll a concentration and high-resolution SST were taken from the ERDDAP NOAA CoastWatch server at <https://coastwatch.noaa.gov/erddap/griddap/index.html?page=1&itemsPerPage=1000>.

Statistical calculation and analysis of the spatio-temporal variability of the used data characteristics were carried out according to a unified methodology [29]. Taking into account the duration of the summer and winter monsoons and the intra-annual cycle of T_a and SST, conditionally warm, summer (June – September), and conditionally cold, winter (November – March), seasons (periods) of the year were selected. Calculations were carried out both for the entire 42-year period of 1982–2023 and for its first (1982–2002) and second (2003–2023) halves. The 95% significance level for trends in time series and correlation coefficients was assessed using Student's t -test with effective degrees of freedom.

A wind-based upwelling index allowing for quantitative estimates of the offshore-directed Ekman transport in the surface friction layer [30] was used to study the possibility of manifestation and characteristics of seasonal coastal upwelling in the study area. The index was calculated from the wind field in coastal ocean areas using the data obtained from satellite scatterometers, which capture the short-period variability of the wind field [31]. For the coastal areas of the southeastern coast of Kamchatka and Avacha Gulf, the equation for calculating the wind-based upwelling index can be presented as follows:

$$UI = -Q_x \sin(a - \pi/2) + Q_y \cos(a - \pi/2),$$

where a is the angle between the corresponding parallel and the straight line approximating the average coastline; Q_x and Q_y are the values of the zonal and meridional components of the wind-driven transport. In this case, $Q_x = \tau_y/\rho f$, $Q_y = -\tau_x/\rho f$, where τ_x and τ_y are the values of the zonal and meridional components of the wind stress, ρ is the density of seawater (1025 kg·m⁻³), f is the Coriolis parameter. Wind stress was calculated using the equations proposed in [32].



Warming trends in the waters off the eastern coast of the Kamchatka Peninsula and adjacent areas

Overall, a statistically significant positive trend in mean annual SST anomalies (ΔT) was observed for the region during 1982–2023, amounting to 0.31°C per decade. The anomaly and cumulative anomaly plots reveal two distinct phases (periods) of climatic change: 1982–2002, characterized by predominantly negative SST anomalies, and 2003–2023, characterized by predominantly positive anomalies (Fig. 1, *a, b*).

The mean annual SST trend value in the first phase was 0.02°C per decade and was not statistically significant, whereas in the second phase it increased to a significant 0.36°C per decade. During the warm period of the year in the first phase (1982–2002), a moderate increase in SST of up to 0.12°C per decade was observed across the entire region. However, in the subsequent period (2003–2023), the SST trend sharply intensified, reaching 0.64°C per decade. This is associated with a transition to a new climatic regime and changes in atmospheric circulation characteristics in the region. Moreover, as previously shown [26], the identified trends also differ in the northern and southern sectors of the waters throughout the extratropical zone of the northwestern Pacific Ocean. As seen in Fig. 1, *c–f*, in the last two decades, the sign of the SST trend in the waters of the western and northwestern parts of the study area changed from negative to positive. Furthermore, during the warm period of the year, a band of extreme SST trends formed off the coast of the eastern part of the Kamchatka Peninsula (Fig. 1, *f*), which, according to our estimates, reached unprecedented values for the entire Pacific basin – up to 1.45°C per decade.

Average characteristics of marine heat waves

Fig. 2 shows the temporal changes in some MHW characteristics across the entire region. Over the last 40 years, the figure indicates a gradual increase in the area of the water body affected by this process (number of grid points, N_g – Fig. 2, *c*). These events are recorded throughout all months of the year; however, a sharp increase in their number was observed mid-period (Fig. 2, *d, e*). Overall, the total number of MHW events (N_e) at grid points over this period increased from 213 in 1987 to 19.7 thousand in 2018 (an average of ~ 6.5 thousand events per year occurred during the period), showing a significant trend of ~ 3.5 thousand events per decade. The amplitude-frequency characteristics of the intra-annual dynamics of these events also vary across the region and exhibit specific features depending on the year within each period (Fig. 2, *a, b*). The interannual course of the N_e curve reflects the general warming trends in the region and two main periods marking key climate changes (Fig 1, *a*; 2, *d*).

The main peaks on this curve correspond to peak El Niño values that occurred in recent decades, and the overall trend coincides with global climate changes [1, 29, 33]. Further analysis of MHW characteristics in the region focused on the most recent 20-year time interval (2003–2023). Fig. 3 shows the frequency of events, their duration, intensity, and integral indices, highlighting significant regional differences in these indicators over the last two decades.

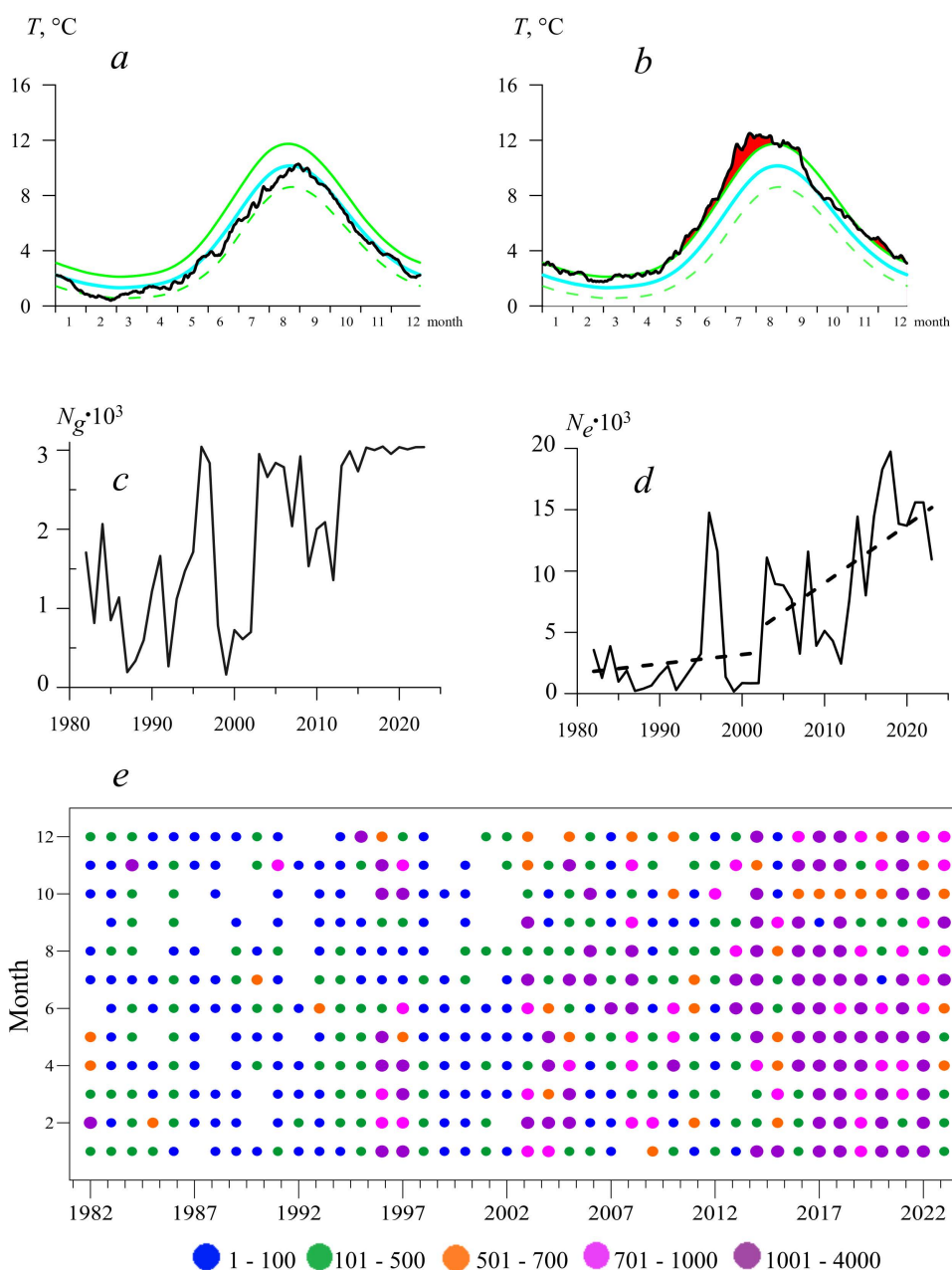


Fig. 2. General indicators of MHW events in the region under study. Changes of daily average SST (black curve), climatological average SST (blue curve), and the 90th (solid green curve) and 10th (dashed green curve) percentile thresholds in 2002 (*a*) and 2023 (*b*); number of grid nodes N_g (*c*) where the MHW events were observed, and a number of MHW events N_e at the grid nodes (*d*); differentiated changes in the number of MHW events over the entire region for different years by months (*e*)

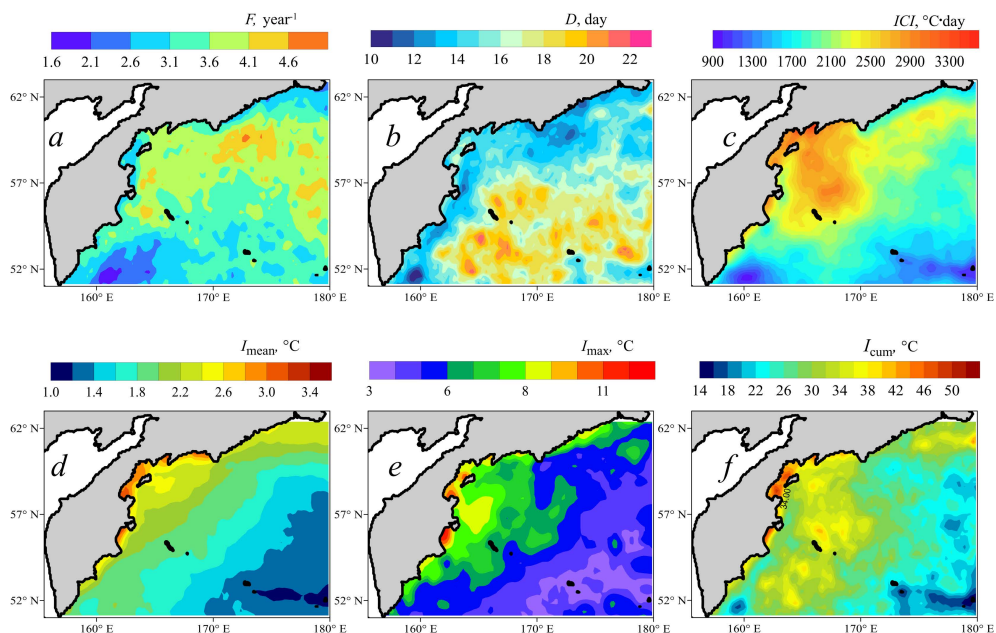


Fig. 3. Spatial distribution of long-term averaged annual mean MHW characteristics in 2003–2023: MHW events frequency (*a*); duration (*b*); composite intensity index (*c*); mean (*d*), maximum (*e*) and cumulative (*f*) intensities

The zone with the lowest frequency of MHW events (fewer than two per year) is located southeast of Kamchatka in the open ocean part, while the highest frequency (more than four per year) was observed near the shelf edge of the Bering Sea (Fig. 3, *a*), as previously noted [34]. The mean event frequency (F) was 3.4 per year. The mean duration of each MHW event (D) in the region's waters was 16 days. However, the duration of these events increases with distance from the continent. In the northwest, the duration is 10–12 days, whereas in the deep-water areas of the southeastern part of the region, it is 20–25 days (Fig. 3, *b*).

Over 20 years, the mean and maximum mean of MHW intensities in the study area were 1.8 °C and 5.2 °C, respectively. The mean cumulative intensity was 28.2 °C. The highest values of these characteristics ($I_{\text{mean}} \sim 3.4$ °C, $I_{\text{max}} \sim 11.5$ °C and $I_{\text{cum}} \sim 50$ °C) were recorded in a narrow coastal zone in the northeastern part of the Kamchatka Peninsula and in adjacent ocean waters near the continent (Fig. 3, *d–f*). The composite intensity index (ICI), which combines the three main MHW variables (F , D , I_{mean}), provides a more comprehensive picture of MHW manifestation. The spatial distribution of the ICI (Fig. 3, *c*) shows higher index values in the western Bering Sea basin and lower values in the southern region.

These general trends in the dynamics of daily MHW characteristics, on the one hand, are an expected consequence of rising mean ocean surface temperature under global warming [33], and on the other hand, reflect selective sensitivity to sea surface temperature changes and may serve as both precursors to and causes of interannual temperature fluctuation trends [34].

Interannual and seasonal changes in MHWs

Fig. 4 shows the interannual changes in the main characteristics of MHWs, averaged across the entire study area. MHW indicators exhibit peak values towards the end of the 1982–2023 period. A positive linear trend is clearly visible (Fig. 4, table). The relationships between changes in MHW characteristics, anomalies of various regional climate indicators, and climate indices demonstrate relatively close correlations.

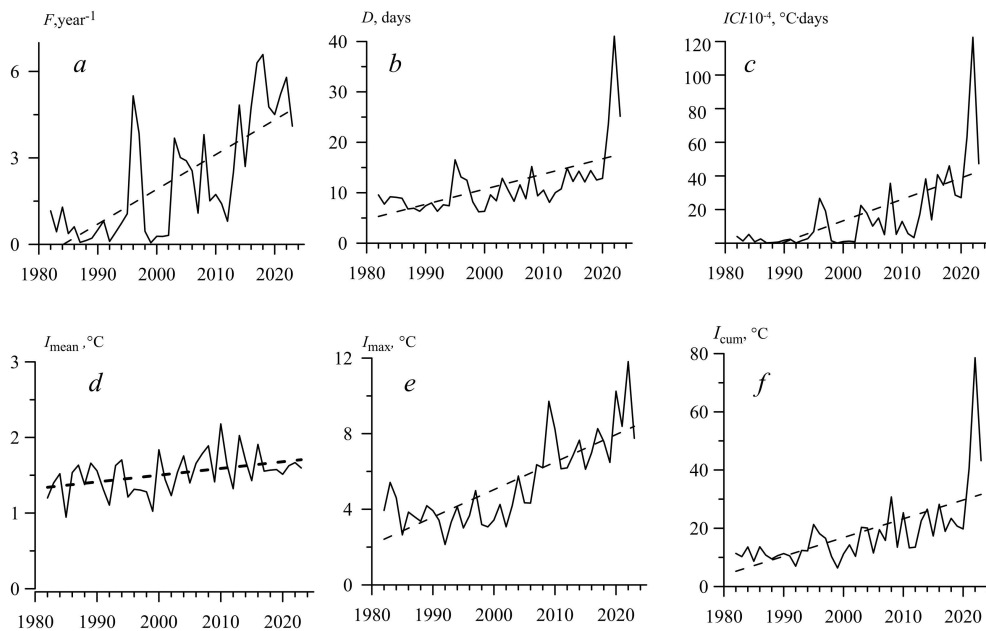


Fig. 4. Regionally averaged annual mean values of frequency F (a), duration D (b), composite intensity index ICI (c), mean I_{mean} (d), maximum I_{max} (e) and cumulative I_{cum} (f) intensities of MHW events for 1982–2023. Legend: solid line denotes MHW index, dashed line – linear trend

Trends in MHW indicators across the region are characterized by the following features. The number of MHW events per year increases by 1.2 per decade (table). The mean duration of each event increased by 3.7 days per decade, reaching a record 49 days in 2022 (Fig. 4, b). This explains the presence of peaks in the distribution of cumulative intensity (Fig. 4, f) and the composite MHW index for that year (Fig. 4, c). On average, the largest water temperature anomalies relative to climatic norms increased by 1.5 °C per decade (table), consistent with the findings of other studies [33]. The dependence of MHW event duration on their frequency and maximum intensity is characterized by a high correlation ($R = 0.6$).

The data in the table show the presence of average statistically significant correlations between the interannual fluctuations of various MHW indicators and the characteristics of changes in surface air temperature anomalies (overall for the region ($R = 0.61$), T_a anomalies at the nearest coastal meteorological station ($R = 0.61$), geopotential height at the 500 mb level ($R = 0.50$)), as well as with various climate indices. Trends in interannual changes of CIs are mainly

determined by the position, intensity, and interaction of the main baric formations, which are seasonal centers of atmospheric action, and depend on the selected time period. Correlations between fluctuations of *AMO* – *IPO* indices reflect the influence of various large-scale processes, which are part of the global climate variability regime, on the structure of pressure, wind fields, and thermal conditions in the subarctic region through long-range relations [26].

Inter-annual trend (*b*/10 years) values of annual average MHW indicators, and correlation coefficients (*R*) of MHW events with climatic parameters for 1982–2023

Parameters	<i>F</i>	<i>D</i>	<i>ICI</i>	<i>I</i> _{mean}	<i>I</i> _{max}	<i>I</i> _{cum}
<i>b</i>	1.2	3.7	12.5×10³	0.1	1.5	6.4
<i>R</i> / <i>SST</i> _a	0.81	0.57	0.76	0.33	0.55	0.59
<i>R</i> / <i>T</i> _a	0.76	0.63	0.74	0.36	0.52	0.65
<i>R</i> / <i>H</i> ₅₀₀	0.52	0.47	0.51	0.38	0.57	0.53
<i>R</i> / <i>AMO</i>	0.35	0.53	0.38	0.44	0.50	0.44
<i>R</i> / <i>SOI</i>	0.22	0.36	0.32	0.29	0.38	0.42
<i>R</i> / <i>NINO.W</i>	0.61	0.45	0.57	0.39	0.69	0.52
<i>R</i> / <i>NPGO</i>	–0.47	–0.31	–0.35	0.12	–0.19	–0.22
<i>R</i> / <i>IPO</i>	–0.21	–0.38	–0.40	–0.23	–0.38	–0.42

N o t e. *SST*_a is annual average anomalies of surface air temperature based on reanalysis data; *T*_a is annual average anomalies of air temperature at the coastal weather station Apuka (Olyutorka) taken from the website <http://portal.esimo.ru/portal/>; *H*₅₀₀ – anomalies of geopotential height of the 500 mbar surface; *AMO* – *IPO* are climatic indices [26, 29]. Statistically significant (95%) estimates are highlighted in bold

As shown in Fig. 5, the maximum number of MHW events on individual days at the region's grid points, on average for 2003–2023, corresponds to events of short duration (5–10 days per year) (Fig. 5, *a*). The largest number of events of various durations is observed during the warm period of the year. In the intra-annual dynamics, the total number of MHW events averaged over the region increased sharply during the second phase of the study period (Fig. 5, *a* – *d*).

Thus, local atmospheric influences are a key factor in MHW variability in the region under consideration. These influences can be modified by large-scale climate variability regimes.

Marine heat waves and the 2020 HAB off the Kamchatka coast

As mentioned earlier, a trend of accelerated warming has been observed in the study waters over the last two decades, and marine heat wave events have

spread throughout the entire region (Figs. 1–4). By the end of this period, MHWs and anomalously high temperatures had severely impacted the biota of the coastal zone and adjacent marine areas. In the context of the Kamchatka ecological disaster of late September – early October 2020, these processes were accompanied by the mass development of microalgae and a significant increase in chlorophyll *a* concentration [18, 19, 21], which apparently contributed to the HAB outbreak. Processes of mixing in the upper ocean layer, which promote the supply of nutrients and dinoflagellates to the photic layer, were also considered among the causes of this phenomenon [18, 19, 21]. One such process is coastal upwelling, which is the rise of deep waters to the surface caused by wind forcing.

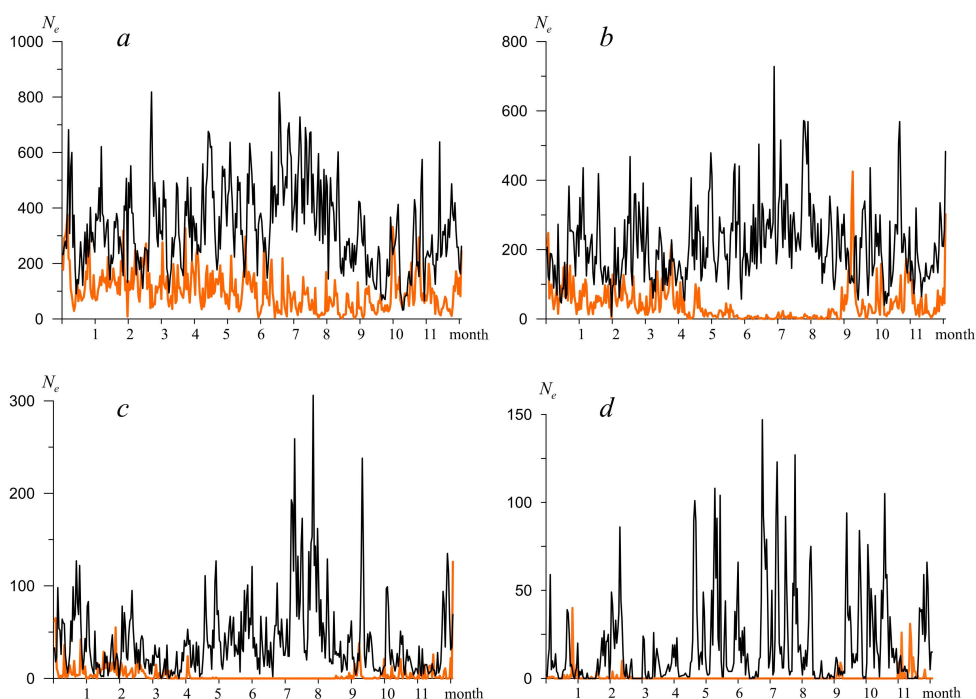


Fig. 5. Number of MHW events (N_e) of different durations for 1982–2002 (orange curve) and 2003–2023 (black curve) averaged for the entire region for different days and seasons of a year: 5–10 days per year (*a*), 11–32 days (*b*), 33–62 days (*c*), and more than 62 days (*d*)

It should be noted that the influence of wind-driven upwelling on the thermal structure of the waters off the eastern coast of the Kamchatka Peninsula during the period of sharp environmental deterioration in September – October 2020 had not been previously studied. To analyze this process, satellite maps of SST distribution can be used. These maps highlight upwelling zones as areas of colder waters near the coast. Additionally, results from calculating the wind-based upwelling index (Fig. 6, *b*, *d*) can be used.

The wind-based upwelling index is used to evaluate the intensity of upwelling in coastal waters. Positive index values indicate upwelling and negative values

indicate downwelling (sinking of waters). Our calculations showed that favorable conditions for the development of seasonal coastal upwelling can form during the summer-autumn period when western and southwestern winds with an average speed of $4\text{--}9\text{ m}\cdot\text{s}^{-1}$ [27] prevail over the coastal strip and the region's waters. Maximum positive upwelling index values in the coastal zone of Kamchatka within the $52\text{--}53^\circ\text{ N}$ latitude band (Fig. 6, *b*) indicate intense upwelling and are observed in fall, following spring-summer MHW events (Fig. 6, *a*). These events are accompanied by the formation of a belt of colder waters in the coastal zone (Fig. 6, *d*), as well as a sharp increase in chlorophyll *a* concentration in the intra-annual course (Fig. 6, *c*) and a change in its spatial distribution (Fig. 6, *f*) compared to periods without pronounced wind-driven upwelling (Fig. 6, *e*). It should be noted that besides the impact of toxins on biota causing the death of marine organisms during HAB outbreaks, another negative factor is the decrease in dissolved oxygen levels to critical values in the bottom layers [11] during the death and decomposition of microalgal biomass. In the context of the Kamchatka ecological disaster, such cases of hypoxia have not been sufficiently studied.

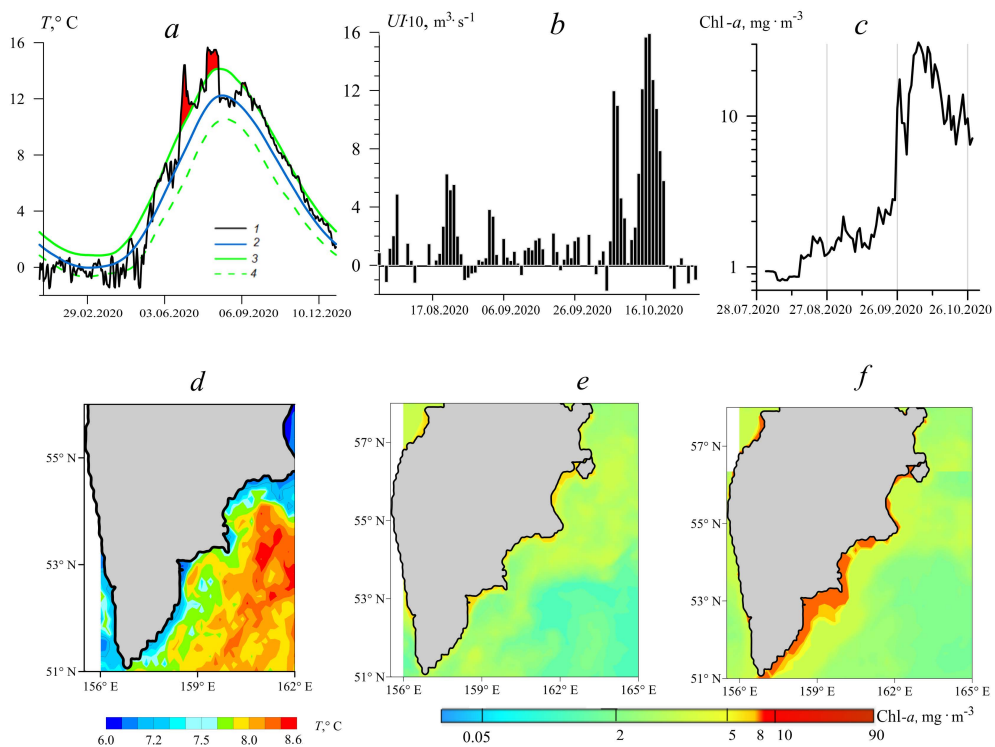


Fig. 6. Changes in daily average SST (1), climatological average SST (2), and the 90th (3) and 10th (4) percentile threshold values in temperature seasonal variation in the study area off the coast of Avacha Gulf in 2020 (*a*); temporal variability of daily upwelling index values in the same area in summer – fall, 2020 (*b*); intra-annual variability of surface chlorophyll *a* concentration off the coast of Avacha Gulf in August – October, 2020 (*c*); SST for 10.28.2020 (*d*); distribution of chlorophyll *a* concentration on the ocean surface on 08.15.2020 (*e*) and 10.15.2020 (*f*)

Conclusion

1. During 1982–2023, extreme marine heat wave phenomena developed and intensified amid positive sea surface temperature trends. Throughout the first 20-year period (1982–2002), the linear trends in interannual changes of SST and various MHW indicators were small and statistically insignificant. In the second phase (2003–2023), these characteristics demonstrated significant positive interannual trends, confirming the steady intensification of MHW phenomena in terms of event frequency, duration, intensity, and integral indices, highlighting significant regional differences in these indicators over the past few decades.

2. The number of MHW events increased from 213 in 1987 to 19.7 thousand in 2018, corresponding to a significant trend of 3.5 thousand events per decade. On average, ~ 6.5 thousand such events occurred per year in the region, with peaks coinciding with El Niño phases. The maximum number of MHW events on individual days corresponded to a short duration (5–10 days per year). The mean event frequency was 3.4 per year, and the mean event duration was 16 days. In 2003–2023, the highest values of various MHW indicators were recorded in the narrow coastal zone of northeastern Kamchatka and its adjacent waters.

3. Statistically significant correlations were identified between the fluctuations of various MHW indicators and the changes in the characteristics of surface air temperature anomalies, geopotential height of the 500 mb isobaric surface, as well as climate indices (*AMO*, *NINO.WEST*, *NPGO* and *IPO*), indicating the influence of air temperature field anomalies and large-scale atmospheric processes on MHW development.

4. During the HAB outbreak off the Kamchatka coast, wind-driven upwelling intensified in the coastal zone, promoting the supply of nutrients and dinoflagellates to the photic layer. The conducted research supports the hypotheses that upwelling played an important causal role in the chain of events that led to the ecological disaster in the study region in fall 2020.

REFERENCES

1. WMO, 2024. *State of the Global Climate 2023*. World Meteorological Organization. WMO-No. 1347. WMO, 48 p.
2. Hobday, A.J., Alexander, L.V., Perkins, S.E., Smale, D.A., Straub, S.C., Oliver, E.C.J., Benthuisen, J.A., Burrows, M.T., Donat, M.G. [et al.], 2016. A Hierarchical Approach to Defining Marine Heatwaves. *Progress in Oceanography*, 141, pp. 227-238. <https://doi.org/10.1016/j.pocean.2015.12.014>
3. Oliver, E.C.J., Benthuisen, J.A., Darmaraki, S., Donat, M.G., Hobday, A.J., Holbrook, N.J., Schlegel, R.W. and Sen Gupta, A., 2021. Marine Heatwaves. *Annual Review of Marine Science*, 13(1), pp. 313-342. <https://doi.org/10.1146/annurev-marine-032720-095144>
4. Vogt, L., Burger, F.A., Griffies, S.M. and Frölicher, T.L., 2022. Local Drivers of Marine Heatwaves: A Global Analysis with an Earth System Model. *Frontiers in Climate*, 4, 847995. <https://doi.org/10.3389/fclim.2022.847995>
5. Yao, Y., Wang, C. and Fu, Y., 2022. Global Marine Heatwaves and Cold-Spells in Present Climate to Future Projections. *Earth's Future*, 10(11), e2022EF002787. <https://doi.org/10.1029/2022EF002787>

6. He, Y., Shu, Q., Wang, Q., Song, Z., Zhang, M., Wang, S., Zhang L., Bi, H., Pan, R. and Qiao F., 2024. Arctic Amplification of Marine Heatwaves under Global Warming. *Nature Communication*, 15(1), 8265. <https://doi.org/10.1038/s41467-024-52760-1>
7. Joyce, P.W.S., Tong, C.B., Yip, Y.L. and Falkenberg, L.J., 2024. Marine Heatwaves as Drivers of Biological and Ecological Change: Implications of Current Research Patterns and Future Opportunities. *Marine Biology*, 171(1), 20. <https://doi.org/10.1007/s00227-023-04340-y>
8. Bian, C., Jing, Z., Wang, H. and Wu, L., 2024. Scale-Dependent Drivers of Marine Heatwaves Globally. *Geophysical Research Letters*, 51(3), e2023GL107306. <https://doi.org/10.1029/2023gl107306>
9. Le Grix, N., Zscheischler, J., Rodgers, K.B., Yamaguchi, R. and Frölicher, T.L., 2022. Hotspots and Drivers of Compound Marine Heatwaves and Low Net Primary Production Extremes. *Biogeosciences*, 19(24), pp. 5807-5835. <https://doi.org/10.5194/bg-19-5807-2022>
10. Frölicher, T.L. and Laufkötter, C., 2018. Emerging Risks from Marine Heat Waves. *Nature Communications*, 9(1), 650. <https://doi.org/10.1038/s41467-018-03163-6>
11. Anderson, D.M., Fensin, E., Gobler, C.J., Hoeglund, A.E., Hubbard, K.A., Kulis, D.M., Landsberg, J.H., Lefebvre, K.A., Provoost, P. [et al.], 2021. Marine Harmful Algal Blooms (HABs) in the United States: History, Current Status and Future Trends. *Harmful Algae*, 102, 101975. <https://doi.org/10.1016/j.hal.2021.101975>
12. Falkowski, P.G. and Oliver, M.G., 2007. Mix and Match: How Climate Selects Phytoplankton. *Nature Reviews: Microbiology*, 5(10), pp. 813-819. <https://doi.org/10.1038/nrmicro1751>
13. Krishnapriya, M.S., Varikoden, H., Anjaneyan, P. and Kuttippurath, J., 2023. Marine Heatwaves during the Pre-Monsoon Season and Their Impact on Chlorophyll-a in the North Indian Ocean in 1982–2021. *Marine Pollution Bulletin*, 197, 115783. <https://doi.org/10.1016/j.marpolbul.2023.115783>
14. Noh, K.M., Lim, H.-G. and Kug, J.-S., 2022. Global Chlorophyll Responses to Marine Heatwaves in Satellite Ocean Color. *Environmental Research Letters*, 17(6), 064034. <https://doi.org/10.1088/1748-9326/ac70ec>
15. Kuroda, H., Azumaya, T., Setou, T. and Hasegawa, N., 2021. Unprecedented Outbreak of Harmful Algae in Pacific Coastal Waters off Southeast Hokkaido, Japan, during Late Summer 2021 after Record-Breaking Marine Heatwaves. *Journal of Marine Science and Engineering*, 9(12), 1335. <https://doi.org/10.3390/jmse9121335>
16. Song, N.-Q., Wang, N., Lu, Y. and Zhang, J.-R., 2016. Temporal and Spatial Characteristics of Harmful Algal Blooms in the Bohai Sea during 1952–2014. *Continental Shelf Research*, 122, pp. 77-84. <https://doi.org/10.1016/j.csr.2016.04.006>
17. McCabe, R.M., Hickey, B.M., Kudela, R.M., Lefebvre, K.A., Adams, N.G., Bill, B.D., Gulland, F.M.D., Thomson, R.E., Cochlan, W.P. [et al.], 2016. An Unprecedented Coastwide Toxic Algal Bloom Linked to Anomalous Ocean Conditions. *Geophysical Research Letters*, 43(19), pp. 10366-10376. <https://doi.org/10.1002/2016GL070023>
18. Bondur, V., Zamshin, V., Chvertkova, O., Matrosova, E. and Khodaeva, V., 2021. Detection and Analysis of the Causes of Intensive Harmful Algal Bloom in Kamchatka Based on Satellite Data. *Journal of Marine Science and Engineering*, 9(10), 1092. <https://doi.org/10.3390/jmse9101092>
19. Orlova, T.Y., Aleksanin, A.I., Lepskaya, E.V., Efimova, K.V., Selina, M.S., Morozova, T.V., Stonik, I.V., Kachur, V.A., Karpenko, A.A. [et al.], 2022. A Massive Bloom of *Karenia* Species (Dinophyceae) off the Kamchatka Coast, Russia, in the Fall of 2020. *Harmful Algae*, 120(2), 102337. <https://doi.org/10.1016/j.hal.2022.102337>
20. Kuroda, H., Taniuchi, Y., Watanabe, T., Azumaya, T. and Hasegawa, N., 2022. Distribution of Harmful Algae (*Karenia* spp.) in October 2021 off Southeast Hokkaido, Japan. *Frontiers in Marine Science*, 9, 841364. <https://doi.org/10.3389/fmars.2022.841364>

21. Tskhay, Zh.R. and Shevchenko, G.V., 2022. Distribution Features of Chlorophyll a Concentration off the East Coast of Kamchatka in Autumn 2020 from Satellite Data. *Sovremennyye Problemy Distantionnogo Zondirovaniya Zemli iz Kosmosa*, 19(1), pp. 226-238. <https://doi.org/10.21046/2070-7401-2022-19-1-226-238> (in Russian).
22. Hobday, A.J., Oliver, E.C.J., Sen Gupta, A., Benthuisen, J.A., Burrows, M.T., Donat, M.G., Holbrook, N.J., Moore, P.J., Thomsen, M.S. [et al.], 2018. Categorizing and Naming Marine Heatwaves. *Oceanography*, 31(2), pp. 162-173. <https://doi.org/10.5670/oceanog.2018.205>
23. Spillman, C.M., Smith, G.A., Hobday, A.J. and Hartog, J.R., 2021. Onset and Decline Rates of Marine Heatwaves: Global Trends, Seasonal Forecasts and Marine Management. *Frontiers in Climate*, 3, 801217. <https://doi.org/10.3389/fclim.2021.801217>
24. Lim, Y.K., Park, B.S., Kim, J.H., Baek, S.-S. and Baek, S.H., 2021. Effect of Marine Heatwaves on Bloom Formation of the Harmful Dinoflagellate *Cochlodinium Polykrikoides*: Two Sides of the Same Coin? *Harmful Algae*, 104, 102029. <https://doi.org/10.1016/j.hal.2021.102029>
25. Yao, Y., Wang, J., Yin, J. and Zou, X., 2020. Marine Heatwaves in China's Marginal Seas and Adjacent Offshore Waters: Past, Present, and Future. *Journal of Geophysical Research: Oceans*, 125(3), e2019JC015801. <https://doi.org/10.1029/2019JC015801>
26. Rostov, I.D., Dmitrieva, E.V. and Rudykh, N.I., 2023. Interannual Variability of Thermal Characteristics of the Upper 1000-meter Layer in the Extratropical Zone of the Northwestern Part of the Pacific Ocean at the Turn of the XX–XXI Centuries. *Physical Oceanography*, 30(2), pp. 141-159. <https://doi.org/10.29039/1573-160X-2023-2-141-159>
27. Rostov, I.D., Dmitrieva, E.V. and Vorontsov, A.A., 2018. Tendencies of Climate Changes for Thermal Conditions in the Coastal Waters of the Western Bering Sea and Adjacent Areas in the Last Decades. *Izvestiya TINRO*, 193(2), pp. 167-182. <https://doi.org/10.26428/1606-9919-2018-193-167-182> (in Russian).
28. Zhao, Z. and Marin, M., 2019. A MATLAB Toolbox to Detect and Analyze Marine Heatwaves. *The Journal of Open Source Software*, 4(33), 1124. <https://doi.org/10.21105/joss.01124>
29. Rostov, I.D., Dmitrieva, E.V. and Rudykh, N.I., 2023. Changes in the Thermal Condition Trends in the Tropical Zone of the Pacific Ocean in 1982–2021. *Oceanology*, 63(6), pp. 755-768. <https://doi.org/10.1134/S0001437023060127>
30. Bakun, A., 1990. Global Climate Change and Intensification of Coastal Ocean Upwelling. *Science*, 247(4939), pp. 198-201. <https://doi.org/10.1126/science.247.4939.198>
31. Gonzalez-Nuevo, G., Gago, J. and Cabanas, J.M., 2014. Upwelling Index: A Powerful Tool for Marine Research in the NW Iberian Upwelling System. *Journal of Operational Oceanography*, 7(1), pp. 47-57. <https://doi.org/10.1080/1755876x.2014.11020152>
32. Large, W.G. and Pond, S., 1981. Open Ocean Momentum Flux Measurements in Moderate to Strong Winds. *Journal of Physical Oceanography*, 11(3), pp. 324-336. [https://doi.org/10.1175/1520-0485\(1981\)011<0324:OOMFMI>2.0.CO;2](https://doi.org/10.1175/1520-0485(1981)011<0324:OOMFMI>2.0.CO;2)
33. Cheng, Y., Zhang, M., Song, Z., Wang, G., Zhao, C., Shu, Q., Zhang, Y. and Qiao, F., 2023. A Quantitative Analysis of Marine Heatwaves in Response to Rising Sea Surface Temperature. *Science of The Total Environment*, 881, 163396. <https://doi.org/10.1016/j.scitotenv.2023.163396>
34. Carvalho, K.S., Smith, T.E. and Wang, S., 2021. Bering Sea Marine Heatwaves: Patterns, Trends and Connections with the Arctic. *Journal of Hydrology*, 600, 126462. <https://doi.org/10.1016/j.jhydrol.2021.126462>

Submitted 09.12.2024; approved after review 15.01.2025;
accepted for publication 15.05.2025.

About the authors:

Igor D. Rostov, Leading Researcher, Laboratory of Informatics and Ocean Monitoring, V.I. Il'ichev Pacific Oceanological Institute, Far Eastern Branch of Russian Academy of Sciences
462

(43 Baltiyskaya Str., Vladivostok, 690041, Russian Federation), CSc. (Geogr.), **ORCID ID: 0000-0001-5081-7279**, **Scopus Author ID: 6603588318**, **SPIN-code: 2329-0391**, rostov@poi.dvo.ru

Elena V. Dmitrieva, Senior Researcher, Laboratory of Informatics and Ocean Monitoring, V.I. Il'ichev Pacific Oceanological Institute, Far Eastern Branch of Russian Academy of Sciences (43 Baltiyskaya Str., Vladivostok, 690041, Russian Federation), CSc. (Tech.), **ORCID ID: 0000-0002-0094-5296**, **Scopus Author ID: 36788322900**, **SPIN-code: 6818-1898**, e_dmitrieva@poi.dvo.ru

Igor A. Zhabin, Leading Researcher, Laboratory of Hydrological Processes and Climate, V.I. Il'ichev Pacific Oceanological Institute, Far Eastern Branch of Russian Academy of Sciences (43 Baltiyskaya Str., Vladivostok, 690041, Russian Federation), CSc. (Geogr.), **ORCID ID: 0000-0002-0294-7156**, **Scopus Author ID: 6701652344**, **SPIN-code: 5881-2713**, zhabin@poi.dvo.ru

Contribution of the co-authors:

Igor D. Rostov – development of the article structure, processing and analysis of the data, writing the article text

Elena V. Dmitrieva – collection and processing of oceanographic data, calculations, drawing design, text editing

Igor A. Zhabin – upwelling problem statement and data analysis

The authors have read and approved the final manuscript.

The authors declare that they have no conflict of interest.